IET Intelligent Transport Systems

Research Article

IET Journals
The Institution of Engineering and Technology

Predicting vacant parking space availability: an SVR method with fruit fly optimisation

ISSN 1751-956X
Received on 5th March 2018
Revised 26th June 2018
Accepted on 9th August 2018
E-First on 12th October 2018
doi: 10.1049/iet-its.2018.5031
www.ietdl.org

Junkai Fan[1], Qian Hu[1], Zhenzhou Tang[1] ✉

[1]*College of Mathematics, Physics and Electronic Information Engineering, Wenzhou University, Wenzhou, People's Republic of China*
✉ *E-mail: mr.tangzz@gmail.com*

Abstract: In this study, a novel prediction model for the number of vacant parking spaces after a specific period of time is proposed based on support vector regression (SVR) with fruit fly optimisation algorithm (FOA). In the proposed model, the SVR parameters are initialised as the fruit fly population, and FOA is utilised to search the optimal parameters for SVR. Sufficient experiments within various scenarios, i.e. predicting the vacant parking space availability in parking lots with various capacities after various periods of time, have been conducted to verify the effectiveness of the proposed FOA-SVR prediction model. Three other commonly used prediction models, i.e. backpropagation neural network (NN), extreme learning machine and wavelet NN, are used as the comparison models. The experimental results show that the proposed FOA-SVR method has higher accuracy and stability in all the prediction scenarios.

1 Introduction

At present, many parking assistant tools such as the smartphone apps can display the real-time vacant parking space availability. However, the number of vacant parking spaces changes as the cars enter or leave the parking lot, which obsoletes the parking space information previously acquired. Therefore, people are more willing to learn the parking spaces available at some time in the future instead of real-time information. A precise vacant parking space availability prediction is beneficial to better plan people's trips and improve the utilisation of parking facilities.

The theories and applications on parking space prediction have been widely studied in recent years. In [1], the continuous-time Markov model-based queuing theory is utilised to predict the availability of vacant parking spaces in the next period of time. By combining the wavelet neural network (WNN) model and the largest Lyapunov exponent method, Ji *et al.* [2, 3] proposed a new multi-step prediction model which is capable of improving the accuracy and stability. Another multi-step forward prediction method combining wavelet transform (WT), artificial NN and prediction strategy was proposed in [4]. Compared to many prediction strategies, the multi-step forward prediction method based on WT can effectively improve the prediction accuracy. Leu and Zhu [5] used two common regression schemes – linear regression and support vector regression (SVR) to predict the number of bicycles in Ubike stations to determine the number of available parking spaces. Rajabioun and Ioannou [6] used a time–space-dependent multivariate autoregressive model to predict the availability of vacant parking spaces and recommended the most accessible parking location to drivers at the estimated arrival times. Peng and Li [7] proposed a cost-effective parking space search method through time-varying analysis and prediction of historical data. Yu *et al.* [8] adopted the autoregressive integrated moving average model to predict the unoccupied parking spaces. Zheng *et al.* [9] proposed a prediction mechanism for the parking occupancy rate using three feature sets with selected parameters to illustrate the utility of these features. Furthermore, they analyse the relative strengths of different machine learning methods in using these features for prediction.

In summary, the works mentioned above are mainly based on mathematical analyses or backpropagation (BP) NN class method. Although the mathematical methods are relatively simple and quick, the robustness and fault tolerance are limited when the prediction objects fluctuate rapidly. Prediction methods based on BPNN have strong fault tolerance and robustness. However, the BP's convergence speed is slow and easy to fall into the local minimum. Moreover, the prediction results of BPNN are unstable due to its inherent characteristics.

In light of this, this paper proposed a novel SVR [10] method for predicting the number of vacant parking spaces. Different from existing SVR methods, where parameters are manually determined, we employ fruit fly optimisation algorithm (FOA) [11–13] to find the optimal penalty factor for the SVR model in the proposed prediction method, i.e. the SVR model is optimised by FOA. With low computational complexity, the proposed FOA-SVR method is applicable to parking lots with various sizes and is effective for various times of the day. As far as we know, this is the first work that applies FOA-SVR to predict the number of the vacant parking spaces. Moreover, both single-step prediction and multi-step prediction based on FOA-SVR model are investigated. Experimental results show that our model is capable of achieving considerable high accuracy and stability.

The rest of this paper is organised as follows. In Section 2, the methodology of FOA-SVR model is introduced. In Section 3, we present the experimental results and discussion. Finally, the conclusions are summarised in Section 4.

2 Methodology of FOA-SVR model

2.1 FOA-SVR prediction

SVR with fruit FOA (FOA-SVR) [14] is a regression prediction model, where the penalty factors of SVR are optimised by FOA. The FOA is inspired by the foraging behaviour of fruit fly performing new ways of looking for global optimisation (see Fig. 1). The main difference between the SVR and the traditional regression model is that the loss is calculated only if the absolute error between the predicted value and the actual value is greater than the insensitive factor (ϵ). This means there is an interval with $f(x)$ as the central value and 2ϵ as the width, as shown in Fig. 2. Any prediction of a training sample is considered correct if it falls within this interval. Otherwise, the loss is calculated.

The detailed procedure of the FOA-SVR prediction model is as follows:

Step 1: Data preparation: The actual data set on the number of the vacant parking spaces are divided into two subsets: the training set

and the test set. The maximum and minimum methods are adopted to normalise the data in the training set and the test set as follows:

$$t_k = \frac{t_k - t_{\min}}{t_{\max} - t_{\min}} \tag{1}$$

where t_k is the element for normalisation, $t_{\min}$ and $t_{\max}$ are the maximum element and the minimum element of the set, respectively.

Step 2: The SVR parameters are set as the parameter groups (penalty factor C). The parameter group size, the maximum number of iterations and the initial central position of the parameter group (x_c, y_c) are initialised as well below:

$$\begin{aligned} x_c &= 10\,\text{rand}() \\ y_c &= 10\,\text{rand}() \end{aligned} \tag{2}$$

where the operator returns a uniformly distributed random number in the interval (0, 1).

Step 3: Randomly assigns the direction and the range for the parameter individual to search the optimal parameter

$$\begin{aligned} x_i &= x_c + r\,(\text{rand}() - 0.5) \\ y_i &= y_c + r\,(\text{rand}() - 0.5) \end{aligned} \tag{3}$$

where r is the search range of the parameter individual.

Step 4: For any parameter individual i, calculate the distance $[D(i) = \sqrt{x(i)^2 + y(i)^2}]$ between the parameter individual i and the origin. The reciprocal of $D(i)$ is treated as the penalty factor C_i.

Step 5: For any parameter individual i, calculate the prediction t_i^* with the training data vector $\boldsymbol{t}_i = \{t_{i-m}, t_{i-(m-1)}, \ldots, t_{i-1}\}$ by using SVR

$$t_i^* = \langle \boldsymbol{\omega}_i, \phi(\boldsymbol{t}_i) \rangle + b_i\,. \tag{4}$$

where $\langle \cdot \rangle$ denotes the dot product operation, $\boldsymbol{\omega}_i$ is the weight vector, b_i is the offset term and $\phi(\boldsymbol{t}_i)$ is the mapping function.

The objective of SVR is to find a proper $\boldsymbol{\omega}_i$ and b_i such that t_i^* and t_i are as close as possible. The problem can be modelled to the following optimisation problem:

$$\min_{\omega_i,\, b_i} \left\{ \frac{1}{2} \| \boldsymbol{\omega}_i \|^2 + C_i \sum_{i=1}^{n} \ell_\epsilon(t_i^* - t_i) \right\} \tag{5}$$

where $\| \boldsymbol{\omega}_i \|$ is the norm of $\boldsymbol{\omega}_i$, i.e. $\| \boldsymbol{\omega}_i \|^2 = \langle \boldsymbol{\omega}_i, \boldsymbol{\omega}_i \rangle$, n is the number of data items and ℓ_ϵ is the ϵ-insensitive loss function defined as follows:

$$\ell_\epsilon(t_i^*, t_i) = \begin{cases} 0, & |t_i^* - t_i| \le \epsilon \\ |t_i^* - t_i| - \epsilon, & \text{otherwise} \end{cases} \tag{6}$$

By introducing the relaxation variables ξ_i and ξ_i^* into (5), the unconstraint optimisation problem formulated in (5) is transformed to a constraint optimisation problem as follows:

$$\begin{aligned} &\min_{\omega_i,\, b_i} \left\{ \frac{1}{2} \| \boldsymbol{\omega}_i \|^2 + C_i \sum_{i=1}^{n} (\xi_i + \xi_i^*) \right\} \\ &\text{s.t.} \quad t_i^* - t_i \le \epsilon + \xi_i \\ &\qquad t_i - t_i^* \le \epsilon + \xi_i^* \\ &\qquad \xi_i, \xi_i^* \ge 0, \quad i = 1, 2, \ldots, n \end{aligned} \tag{7}$$

In (7), C_i is used to balance the number of sample points, whose flatness and deviation of the SVR models are greater than ϵ. The optimisation problem presented in (7) is a typical convex quadratic optimisation problem and can be solved by the Lagrange multiplier

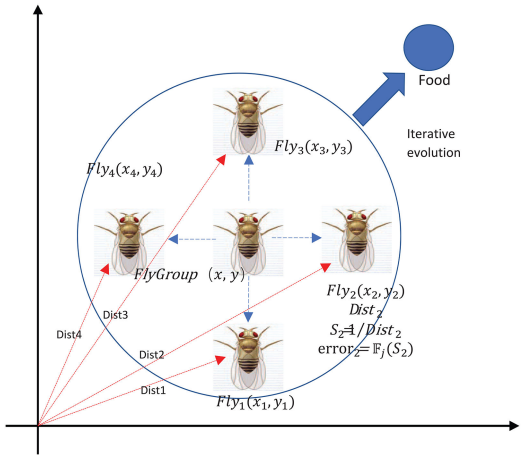

Fig. 1 *Food searching iterative process of a fruit fly swarm*

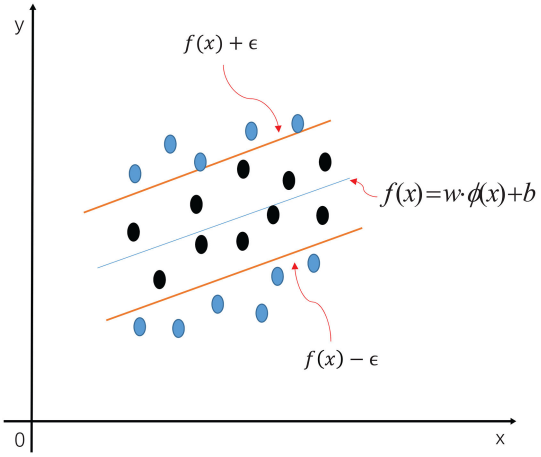

Fig. 2 *SVR diagram*

method. By introducing Lagrange multipliers μ_i, μ_i^*, α_i, α_i^*, the corresponding Lagrangian function is given by

$$\begin{aligned} &L(\omega_i, b, \alpha, \alpha^*, \mu, \mu^*, \xi, \xi^*) \\ &= \frac{1}{2} \| \boldsymbol{\omega}_i \|^2 + C_i \sum_{i=1}^{n} (\xi_i + \xi_i^*) - \sum_{i=1}^{n} \mu_i \xi_i - \sum_{i=1}^{n} \mu_i^* \xi_i^* \\ &+ \sum_{i=1}^{n} \alpha_i (t_i^* - t_i - \epsilon - \xi_i) \\ &+ \sum_{i=1}^{n} \alpha_i^* (t_i - t_i^* - \epsilon - \xi_i^*) \end{aligned} \tag{8}$$

Then, by letting the partial derivatives of L with respect to the primal variables ω, b, ξ_i, ξ_i^* equal to zero, we have

$$\begin{aligned} \boldsymbol{\omega}_i &= \sum_{i=1}^{n} (\alpha_i^* - \alpha_i) \boldsymbol{t}_i \\ 0 &= \sum_{i=1}^{n} (\alpha_i^* - \alpha_i) \\ C_i &= \alpha_i + \mu_i \\ C_i &= \alpha_i^* + \mu_i^* \end{aligned} \tag{9}$$

Substitute (9) into (8), the dual problem of SVR can be expressed as

$$\max_{\alpha,\,\alpha^*} \sum_{i=1}^{n} [t_i(\alpha_i^* - \alpha_i) - \epsilon(\alpha_i^* + \alpha_i) \times -\frac{1}{2}\sum_{i}^{n}\sum_{j}^{n}(\alpha_i^* - \alpha_i)(\alpha_j^* - \alpha_j)\boldsymbol{t}_i^{\mathrm{T}}\boldsymbol{t}_j] \quad \text{s.t.} \sum_{i=1}^{n}(\alpha_i^* - \alpha_i) = 0, \quad 0 \le \alpha_i, \ \alpha_i^* \le C_i \tag{10}$$

According to the Karush–Kuhn–Tucker conditions [15], $\boldsymbol{\omega}_i$ and b_i can be calculated as

$$\boldsymbol{\omega}_i = \sum_{i=1}^{n}(\alpha_i^* - \alpha_i)\phi(\boldsymbol{t}_i) \tag{11}$$

$$b_i = t_i + \varepsilon - \sum_{j=1}^{n}(\alpha_j^* - \alpha_j)\boldsymbol{t}_j^{\mathrm{T}}\boldsymbol{t}_i \tag{12}$$

Substitute (11), (12) into (5), the regression function is written as

$$t_i^* = \sum_{i=1}^{n}(\alpha_i^* - \alpha_i)k(\boldsymbol{t}_i, \boldsymbol{t}_j) + t_i + \epsilon - \sum_{j=1}^{n}(\alpha_j^* - \alpha_j)\boldsymbol{t}_j^{\mathrm{T}}\boldsymbol{t}_i \tag{13}$$

where $k(\boldsymbol{t}_i, \boldsymbol{t}_j) = \phi(\boldsymbol{t}_i)\phi(\boldsymbol{t}_j)$ is a kernel function. $k(\boldsymbol{t}_i, \boldsymbol{t}_j)$ is a symmetric positive real number function which satisfies the *Mercer* theorem. The proposed algorithm uses linear kernel function as the kernel function of the SVR model

$$k(\boldsymbol{t}_i, \boldsymbol{t}_j) = \boldsymbol{t}_i^{\mathrm{T}}\boldsymbol{t}_j \tag{14}$$

In general, any positive semi-definite functions that satisfy Mercer's condition can be used as the kernel function. Table 1 shows some kernel functions for SVR, among which the two most widely used ones are the polynomial kernel and the radial basis function (RBF). As far as we know, so far there is no theoretical basis for the selection of kernel functions for SVR. The kernel functions and parameters are mainly selected by experimental comparisons. For the choice of the kernel function, the RBF kernel function and linear kernel function are more commonly used. The experimental results of RBF kernel function are more dependent on C and γ, while the linear kernel function only needs to optimise C, and the linear kernel function has the advantage of fast operation, but the specific choice is based on the experimental results. In this paper, the proposed FOA-SVR model uses the linear kernel function as the kernel function.

Step 6: For any parameter individual i, calculate the mean-squared error (MSE) between t_i and t_i^* as follows:

$$\mathrm{MSE}_i = \frac{1}{n}\sum_{i=1}^{n}(t_i^* - t_i)^2 \tag{15}$$

The parameter individual with the minimum MSE is selected as the optimal one. Its coordinate becomes the new central position (x_c, y_c).

Step 7: Repeat steps 3–6 and *replace* the optimal parameter individual and the central position if a better one (with smaller MSE) is found in the current round. Stop the iteration if the ending condition is satisfied, i.e. the number of iterations reaches its limit. Thus far, the training process is completed and the optimal penalty factor C_{opt} can be obtained.

Step 8: Substitute C_{opt} into the SVR *model* to predict the number of vacant parking spaces with the test data set.

The computational complexity of the FOA-SVR model depends on the number of training samples (w), the population number (p), the number of generations (g) and scale of the problem (s). So the final computational complexity of the FOA-SVR method is $O(\mathrm{FOA-SVR}) \simeq O(P \times S \times O(W^3)) + g \times (O(P \times S \times O(W^3)))$.

Table 1 Common kernel functions

Kernel types	Kernel functions
linear kernel	$K(\boldsymbol{t}_i, \boldsymbol{t}_j) = (\boldsymbol{t}_i^{\mathrm{T}}\boldsymbol{t}_j)$
polynomial kernel[a]	$K(\boldsymbol{t}_i, \boldsymbol{t}_j) = (\boldsymbol{t}_i^{\mathrm{T}}\boldsymbol{t}_j + 1)^d$
radial-based kernel (RBF)[b]	$K(\boldsymbol{t}_i, \boldsymbol{t}_j) = \exp(-\gamma \parallel \boldsymbol{t}_i - \boldsymbol{t}_j \parallel^2)$
sigmoid kernel	$K(\boldsymbol{t}_i, \boldsymbol{t}_j) = \tanh((\boldsymbol{t}_i^{\mathrm{T}}\boldsymbol{t}_j) + b)$

[a] d is the polynomial order.

[b] γ is the predefined parameter controlling the width of the RBF.

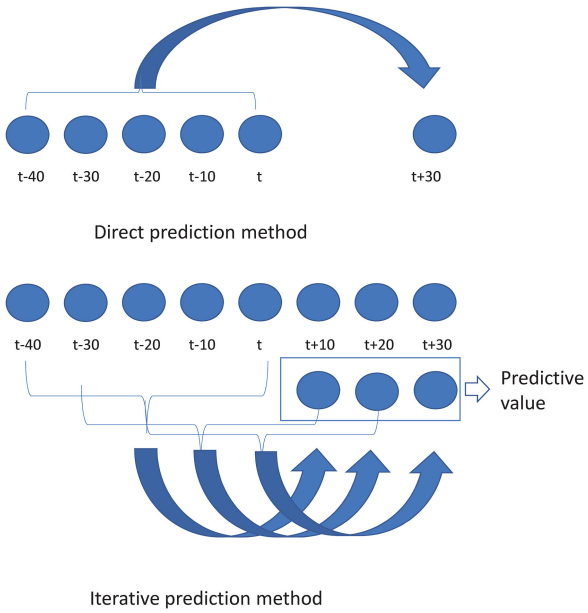

Fig. 3 *Multi-step prediction method*

2.2 Multi-step prediction method

The vacant parking space availability prediction can be classified into single-step prediction and multi-step prediction.

The single-step prediction predicts $t_{T_c+\delta}^*$, where T_c represents the current time point and δ is the time step size by using m historical observations $[t_{T_c}, t_{T_c-\delta}, \ldots, t_{T_c-m\delta}]$, whereas the multi-step prediction predicts $t_{T_c+h\delta}^*(h > 1)$. For example, in single-step prediction, the prediction model predicts the number of vacant parking spaces at $T + 10$ by information at $[T - 40, T - 30, \ldots, T]$. While in the case of multi-step prediction, the prediction model predicts the number of the vacant parking spaces at $T + 30$ with the same information.

Two different multi-step prediction strategies are realised in this paper, i.e. iterative multi-step prediction and direct multi-step prediction. In iterative multi-step prediction, $t_{T_c+\delta}^*$ is first predicted. Moreover then, $t_{T_c+2\delta}^*$ is predicted by $[t_{T_c+\delta}^*, t_{T_c}, \ldots, t_{T_c-(m-1)\delta}]$ in an iterative way. $t_{T_c+2\delta}^*$ is further utilised to predict $t_{T_c+3\delta}^*$, and so on, as shown in Fig. 3. By contrast, direct multi-step prediction outputs the decision on $t_{T_c+h\delta}^*$ directly with historical observations $[t_{T_c}, t_{T_c-\delta}, \ldots, t_{T_c-m\delta}]$. The main procedure of direct multi-step prediction is the same as the single-step prediction.

3 Experimental performance

3.1 Data description

The data on the number of the vacant parking spaces of two parking lots, i.e. the large-capacity parking lot of a local grand shopping mall and the small-capacity parking lot of a restaurant, have been collected. The grand shopping mall represents a scenario

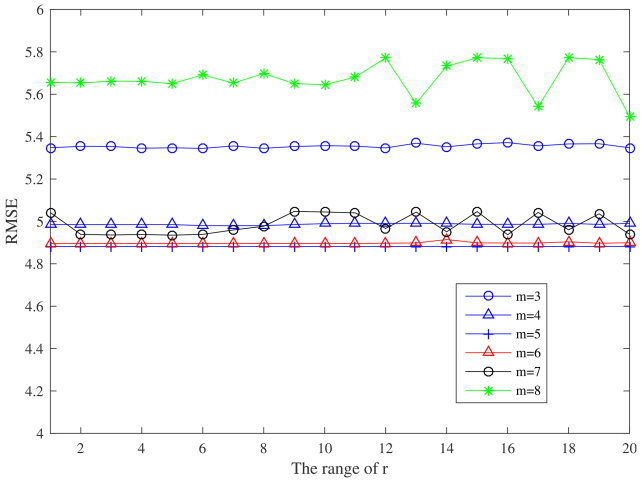

Fig. 4 *Effects of r and m on prediction*

with heavy traffic and obvious traffic flow trends. While the restaurant represents a place with light traffic. Although the traffic flow of the restaurant parking lot also fluctuates up and down, but it is not so obvious. So we believe that these two parking lots are able to represent the traffic condition of most parking lots. For each parking lot, the data were recorded every 10 min from 11 am to 8 pm for two consecutive days. Altogether 108 data items have been collected in 2 days. The first 54 items collected in the first day were used as the training data set and the left 54 items obtained in the following day were included in the test data set.

3.2 Evaluation of indicators

The following indicators are used to show the fitting degrees between the predictions and the actual values in this paper: root MSE (RMSE), mean absolute error (MAE), equalisation coefficient (EC) [16], mean relative error (MRE) and standard deviation (SD). Here, the EC shows the degree of fitting between the predicted value and the actual value, the closer the value is to 1, the better the fitting degree and the higher the prediction accuracy

$$\mathrm{RMSE} = \sqrt{\frac{1}{n}\sum_{i=1}^{n}(t_i^* - t_i)^2} \tag{16}$$

$$\mathrm{MAE} = \frac{1}{n}\sum_{i=1}^{n}|t_i^* - t_i| \tag{17}$$

$$\mathrm{EC} = 1 - \frac{\sqrt{\sum_{i=1}^{n}(t_i^* - t_i)^2}}{\sqrt{\sum_{i=1}^{n}(t_i^*)^2} + \sqrt{\sum_{i=1}^{n}(t_i)^2}} \tag{18}$$

$$\mathrm{MRE} = \frac{1}{n}\sum_{i=1}^{n}\left|\frac{t_i^* - t_i}{t_i^*}\right| \tag{19}$$

$$\mathrm{SD} = \sqrt{\frac{1}{N}\sum_{i=1}^{N}(\mathrm{RMSE}_i - \overline{\mathrm{RMSE}})} \tag{20}$$

where t_i and t_i^* are the actual value and the prediction, respectively; N is the number of experiments. $\overline{\mathrm{RMSE}}$ is the average RMSE of N experiments.

3.3 Experimental setup

Three commonly used prediction algorithms, i.e. BPNN, extreme learning machine (ELM) [17, 18] and WNN [19, 20] are used as the comparison algorithms.

The parameters of the comparison algorithms are set as follows: for SVR without FOA, the penalty factor C is manually set as 0.1, the insensitive factor ϵ is with the default value of 0.1 which is the same as that in SVR-FOA, and the linear kernel function is adopted. For BPNN, the number of hidden layer nodes is 9, the number of iterations is 1000 and the allowable range for the iteration error is 0.0003. For ELM, the number of hidden layer nodes is 9 and the excitation function is sigmod. Moreover for WNN, the number of hidden layer nodes is 6, the weight learning rate is 0.01, the learning rate of the wavelet basis function parameter is 0.008 and the number of iterations is 1000. Moreover, in WNN, the Morlet function is used as the mother wavelet function; the Morlet function can be formulated as

$$y = \cos(1.75x) \times \exp\left(-\frac{x^2}{2}\right) \tag{21}$$

For FOA, the number of iterations is 100 and the population size is 20. The connection weights and thresholds of FOA-BP, FOA-ELM and FOA-WNN are optimised by FOA.

3.4 Experimental results and discussion

The experiment first investigates the effect of the range (r) which is used to assign the random position of a parameter individual in FOA and the number of previous observations m on prediction accuracy. The results are depicted in Fig. 4. It can be observed that r has a very limited effect on the RMSE, whereas m is essential for the effectiveness of prediction. In detail, high predictive performance is achieved when $m = 5$ and 6, whereas a larger or a smaller m both increases the RMSE. That is because a too small m results in insufficient feature extraction and a too large m diminishes the time relativity.

Table 2 shows the comparisons on prediction performances between the direct multi-step prediction and iterative multi-step prediction. The number of the vacant parking spaces after 20 min of the large-capacity parking lot is taken as the predictive object. We can see that though the error accumulates in the process of iteration, the iterative multi-step prediction is superior to the direct multi-step prediction both in prediction accuracy and stability. Therefore, the iterative prediction strategy is adopted in the multi-step prediction in this paper.

Table 3 shows that the division ratios of the training set and the test set have different effects on the experimental results. In many machine learning applications, the cross-validation is commonly used to deal with the issue of data set division. However, in the application of predicting vacant parking space, the values of the data are time related. The cross-validation will undermine the time correlation of the data. In view of this situation, the direct division is adopted to divide the data set into the training part and the testing part. From Table 3, we can observe that the results obtained in the cases of 5:5 (training set:testing set) and 6:4 are almost the optimal divisions. In consideration of having sufficient data for testing, the ratio of 5:5 is selected.

Fig. 5*a* is the iterative optimisation path of FOA. It depicts the searching route for a global optimal solution from where we can observe that the optimal coordinate of the swarm of the fruit fly is

Table 2 Comparison between direct multi-step prediction and iterative multi-step prediction (large-capacity parking lot, $h = 2$)

Method	EC	MAE	MRE	RMSE	SD (RMSE)
direct	0.9871	14.5408	0.0201	18.8325	0.7224
Iteration	**0.9880**	**13.7011**	**0.0189**	**17.5959**	**0.3009**

Bold values indicate the best results.

Table 3 Comparison of experimental results of training sets and test sets with different division ratios (the average of each evaluation index of 100 experiments)

Train: test	10 min (large-parking lot)				
	EC	MAE	MRE	RMSE	SD (RMSE)
4:6	0.9882	12.3496	0.0174	16.8214	1.2000
5:5	**0.9929**	**7.9890**	**0.0111**	**10.2968**	**0.7395**
6:4	**0.9930**	**7.9808**	**0.0110**	**10.2660**	**0.9797**
7:3	0.9920	8.9763	0.0128	11.3453	1.1620
8:2	0.9894	11.3045	0.0179	13.5224	1.3042

Bold values indicate the best results.

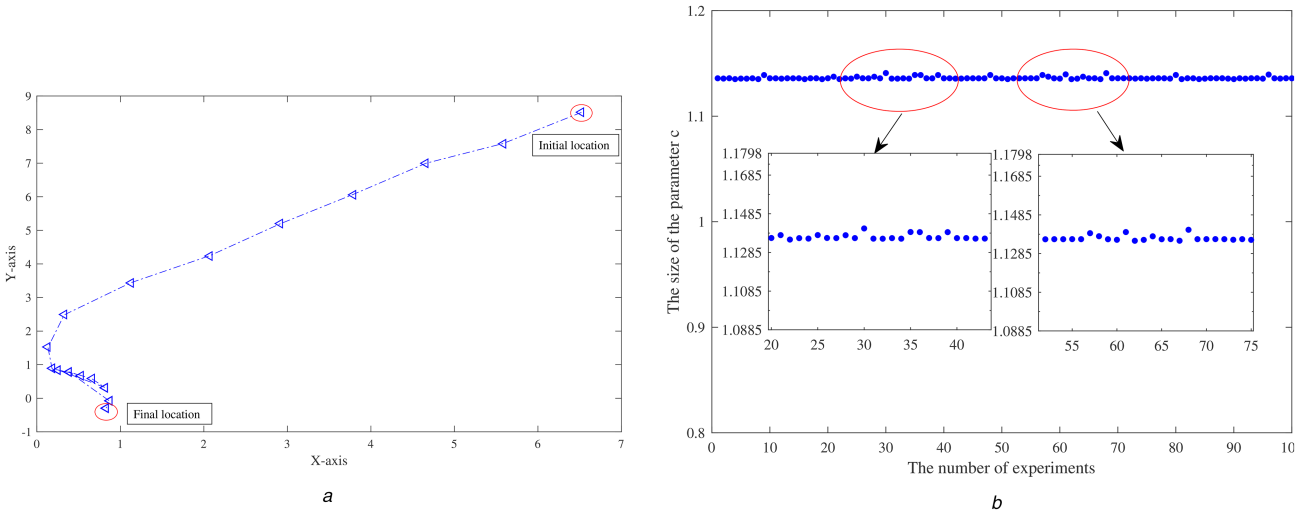

a *b*

Fig. 5 *Effectiveness of FOA*
(a) Referring to parameter optimisation path, ***(b)*** Referring to the effectiveness of FOA

(0.8288, −0.2935). Fig. 5*b* shows the distribution of the penalty factor C. As can be seen from Fig. 5*b*, C slightly fluctuates around 1.136, which shows the effectiveness of the FOA. The reason for the fluctuation may be the premature convergence of the algorithm which makes the searching process fall into local optimums.

Fig. 6 shows the prediction results for two parking lots with different capacities after 10, 20 and 30 min in the future. The predictions and the actual number of the vacant parking spaces are well-fitted, especially for the large-capacity parking lot (EC = 0.9929) for the traffic flow of the large-capacity parking lot located in the grand shopping mall shows a obvious peak–trough characteristics. As for the small-capacity parking lot with less traffic flow, the EC can also achieve 0.9606 though the fitting degree is not as good as a large-capacity parking lot.

Tables 4 and 5 list the results of the prediction performance indicators using SVR, BP, ELM, WNN and their optimisation models (i.e. FOA-SVR, FOA-BP, FOA-ELM and FOA-WNN), respectively. The single-step predictions ($\delta = 10$ min) and the multi-step predictions for the number of the vacant parking spaces 20 and 30 min later are involved. As can be seen from these tables, first, the FOA-SVR achieves higher prediction accuracy in predicting the number of the vacant parking spaces 10, 20 and 30 min later both for the large-capacity parking lot and the small-capacity one. Take the RMSE, which is the most convictive indicator for the performance of accuracy, as an example. The corresponding RMSEs of the FOA-SVR model are 10.2968, 17.5959 and 28.2647, respectively, for the large-capacity parking lot, and 4.9056, 7.0198 and 8.7172, respectively, for the small-capacity one. They are all the lowest among the four prediction models.

We can also observe that though the performances of BP, ELM and WNN are, respectively, improved by exploiting FOA optimisation, FOA-SVR does outperform all the other methods regardless of whether they are optimised by FOA or not, especially in the scenarios with a large-capacity parking lot. Moreover, we can also find that the SD (RMSE) of SVR without FOA is zero. This is because the parameters of SVR without FOA optimisation are fixed, with which the SVR can be formalised as a convex quadratic programming problem and always obtains the same global optimal solution.

4 Conclusions

In this paper, we have proposed a vacant parking space availability prediction model by using the SVR. The penalty factor, which is a key parameter in SVR, is optimised by the fruit fly optimised algorithm in the proposed model. The single-step prediction is used to predict the number of the vacant parking spaces δ minutes later in the future, and the iterative multi-step prediction is used to predict the vacant parking space availability $h\delta (h > 1)$ minutes later in the future. To extensively verify the effectiveness of the proposed FOA-SVR model, we have compared the prediction results with the actual vacant parking spaces in two parking lots with various capacities. The results show that the predictions and the actual vacant parking spaces are well-fitted, especially for the large-capacity parking lot. We also have compared the performance of the proposed FOA-SVR model with other commonly used prediction models (i.e. BP, ELM and WNN) and their optimisation models (i.e. FOA-SVR, FOA-BP, FOA-ELM and FOA-WNN).

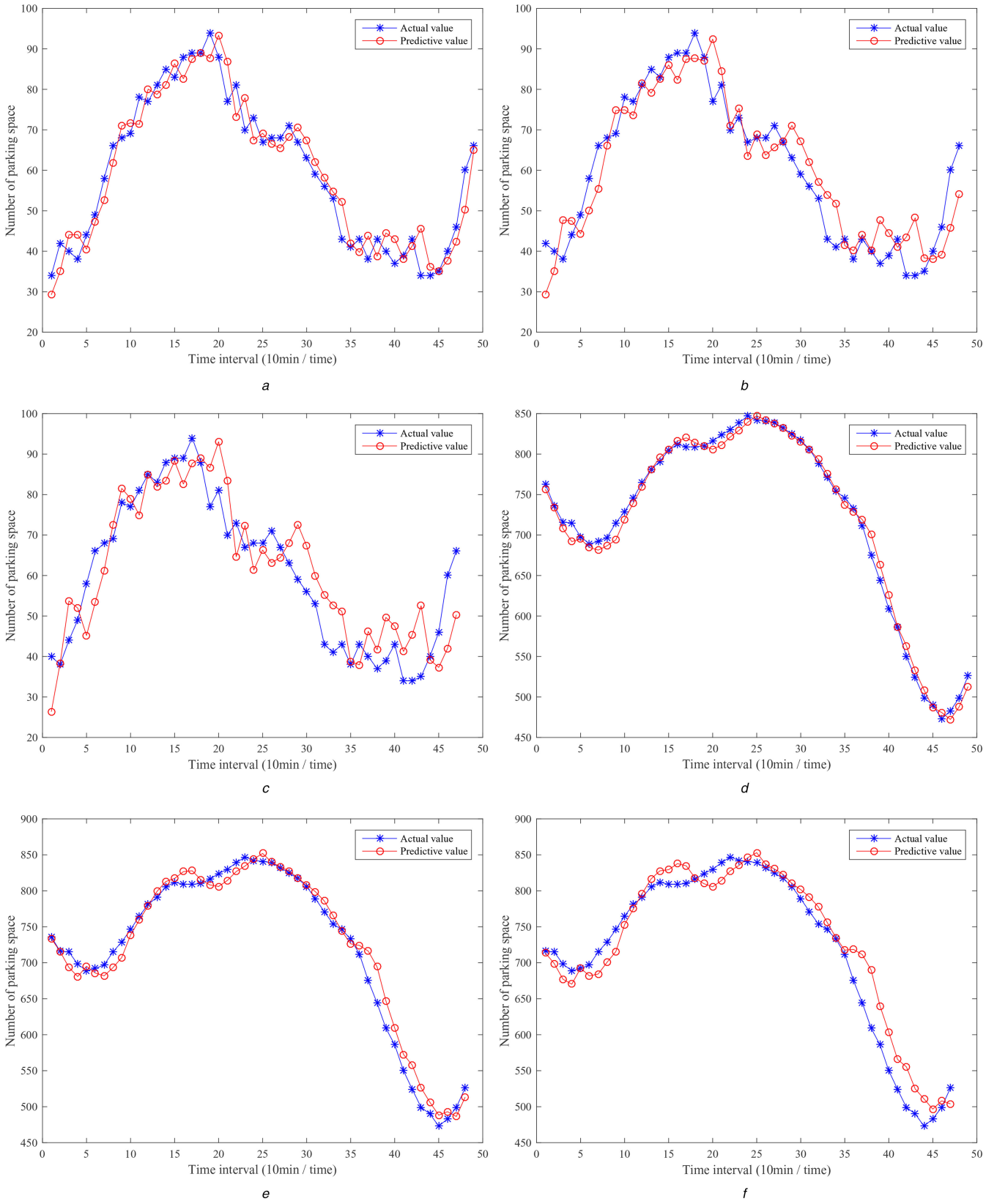

Fig. 6 *Effectiveness of FOA-SVR in parking lots with different capacities. (a), (b), (c) Referring to the effectiveness of FOA-SVR in the large-parking lot. (d), (e), (f) Referring to the effectiveness of FOA-SVR in small-parking lot*
(a) $h = 1$, ***(b)*** $h = 2$, ***(c)*** $h = 3$, ***(d)*** $h = 1$, ***(e)*** $h = 2$, ***(f)*** $h = 3$

The comparison reveals that FOA-SVR outperforms all the other models in accuracy, and it is second only to SVR in stability.

The most essential contribution of our work is the capability of precisely predicting the number of vacant parking spaces. Our prediction model can be applied to any parking lot or garage if only it has the information on vehicle activities such as the time of arrival, departure of vehicles etc. There will be definitely many new intelligent prediction tools in the near future. Moreover, we believe that our prediction model is in line with the future trend of intelligence. In the succeeding work, more environmental factors including the weather, weekday or weekend, time period of data and the surrounding environment etc., can be considered in our prediction model to further improve the accuracy and hence keep the advantages of our model.

Table 4 Average of each evaluation index of 100 experiments (small-capacity parking lot)

Methods	EC	MAE	MRE	RMSE	SD (RMSE)	Methods	EC	MAE	MRE	RMSE	SD (RMSE)
			10 min						10 min		
SVR	0.9560	4.4520	0.0742	5.4806	1.1546×10^{-14}	**FOA-SVR**	**0.9606**	**4.1263**	**0.0693**	**4.9056**	**0.0299**
BP	0.9390	6.1717	0.1055	7.5519	1.7139	FOA-BP	0.9525	4.8703	0.0815	5.9476	0.5263
ELM	0.9564	4.5126	0.0755	5.4448	0.3559	FOA-ELM	0.9567	4.4710	0.0747	5.4085	0.1270
WNN	0.9102	8.3306	0.1398	11.3916	8.3199	FOA-WNN	0.9317	6.8448	0.1212	8.3750	1.6988
			20 min						20 min		
SVR	0.9409	6.0657	0.1016	7.3717	7.9936×10^{-15}	**FOA-SVR**	**0.9443**	**5.5759**	**0.0918**	**7.0198**	**0.1543**
BP	0.9040	9.6807	0.1663	11.9578	1.8774	FOA-BP	0.9234	7.8501	0.1302	9.6998	1.5955
ELM	0.9364	6.4645	0.1069	8.0253	0.4738	FOA-ELM	0.9369	6.3159	0.1048	7.9137	0.3599
WNN	0.8384	16.0811	0.2042	19.9350	11.7427	FOA-WNN	0.9025	10.0072	0.1705	12.2816	2.1661
			30 min						30 min		
SVR	0.9278	7.7208	0.1258	9.1239	7.1054×10^{-15}	**FOA-SVR**	**0.9314**	**7.2794**	**0.1183**	**8.7172**	**0.0435**
BP	0.8699	13.0158	0.2316	16.1506	4.2890	FOA-BP	0.9013	10.4311	0.1678	12.7001	2.2809
ELM	0.9145	8.7974	0.1449	10.8368	0.8161	FOA-ELM	0.9198	8.4649	0.1386	10.1208	0.0757
WNN	0.8214	19.1153	0.1590	23.1391	10.3128	FOA-WNN	0.8778	12.2309	0.2166	15.2229	2.9234

Table 5 Comparison (large-capacity parking lot)

Methods	EC	MAE	MRE	RMSE	SD (RMSE)	Methods	EC	MAE	MRE	RMSE	SD (RMSE)
			10 min						10 min		
SVR	0.9862	16.5888	0.0230	20.2005	3.1974×10^{-14}	**FOA-SVR**	**0.9929**	**7.9890**	**0.0111**	**10.2968**	**0.7395**
BP	0.9830	15.6919	0.0215	24.9684	8.2600	FOA-BP	0.9886	11.3596	0.0156	16.7305	6.2737
ELM	0.9912	9.1643	0.0126	12.8305	4.0885	FOA-ELM	0.9921	8.2057	0.0113	11.5091	3.2429
WNN	0.9686	27.9512	0.0381	46.1848	30.5283	FOA-WNN	0.9705	27.5798	0.0378	43.1609	11.2598
			20 min						20 min		
SVR	0.9807	21.5875	0.0297	28.1315	3.5527×10^{-14}	**FOA-SVR**	**0.9880**	**13.7011**	**0.0189**	**17.5959**	**0.3009**
BP	0.9732	26.4114	0.0360	39.3184	10.4541	FOA-BP	0.9801	21.5893	0.0296	29.1448	5.8239
ELM	0.9837	17.5736	0.0241	23.9351	6.3008	FOA-ELM	0.9853	16.0743	0.0222	21.4224	5.6861
WNN	0.9500	53.7339	0.0749	72.7842	45.1140	FOA-WNN	0.9604	38.7246	0.0537	57.7355	13.4048
			30 min						30 min		
SVR	0.9749	26.9301	0.0369	36.6616	3.5527×10^{-14}	**FOA-SVR**	**0.9807**	**21.7332**	**0.0298**	**28.2647**	**0.3791**
BP	0.9660	35.0664	0.0477	49.9840	9.9465	FOA-BP	0.9738	29.1393	0.0398	38.3732	6.0448
ELM	0.9750	25.6652	0.0350	36.7424	9.8954	FOA-ELM	0.9786	23.9048	0.0328	31.3145	3.2749
WNN	0.9313	78.9820	0.1088	100.7540	49.6311	FOA-WNN	0.9560	45.8486	0.0639	63.9423	14.5476

5 Acknowledgments

This work was supported by the Zhejiang Provincial Natural Science Foundation of China under Grants LY16F010016 and LQ16G010006 and the Graduate Scientific Research Foundation of Wenzhou University.

6 References

[1] Caliskan, M., Barthels, A., Scheuermann, B., *et al.*: 'Predicting parking lot occupancy in vehicular *ad hoc* networks'. 2007 IEEE 65th Vehicular Technology Conf. (VTC), Dublin, Ireland, 2007, pp. 277–281

[2] Ji, Y.J., Tang, D.N., Guo, W.H., *et al.*: 'Forecasting available parking space with largest Lyapunov exponents method', *J. Central South Univ.*, 2014, **21**, (4), pp. 1624–1632

[3] Ji, Y.J., Tang, D., Blythe, P., *et al.*: 'Short-term forecasting of available parking space using wavelet neural network model', *IET Intell. Transp. Syst.*, 2014, **9**, (2), pp. 202–209

[4] Ji, Y.J., Gao, L.P., Chen, X.S., *et al.*: 'Strategies for multi-step-ahead available parking spaces forecasting based on wavelet transform', *J. Central South Univ.*, 2017, **24**, (6), pp. 1503–1512

[5] Leu, J.S., Zhu, Z.Y.: 'Regression-based parking space availability prediction for the Ubike system', *IET Intell. Transp. Syst.*, 2015, **9**, (3), pp. 323–332

[6] Rajabioun, T., Ioannou, P.A.: 'On-street and off-street parking availability prediction using multivariate spatiotemporal models', *IEEE Trans. Intell. Transp. Syst.*, 2015, **16**, (5), pp. 2913–2924

[7] Peng, L., Li, H.: 'Searching parking spaces in urban environments based on non-stationary Poisson process analysis'. 2016 IEEE 19th Int. Conf. Intelligent Transportation Systems (ITSC), Rio de Janeiro, Brazil, 2016, pp. 1951–1956

[8] Yu, F., Guo, J., Zhu, X., *et al.*: 'Real time prediction of unoccupied parking space using time series model'. 2015 IEEE Int. Conf. Transportation Information and Safety (ICTIS), Wuhan, China, 2015, pp. 370–374

[9] Zheng, Y., Rajasegarar, S., Leckie, C.: 'Parking availability prediction for sensor-enabled car parks in smart cities'. 2015 IEEE 10th Int. Conf. Intelligent Sensors, Sensor Networks and Information Processing (ISSNIP), Singapore, Singapore, 2015, pp. 1–6

[10] Drucker, H., Burges, C.J., Kaufman, L., *et al.*: 'Support vector regression machines'. Advances in Neural Information Processing Systems, Denver, CO, USA, 1996, pp. 155–161

[11] Pan, W.T.: 'A new fruit fly optimization algorithm: taking the financial distress model as an example', *Knowl.-Based Syst.*, 2012, **26**, pp. 69–74

[12] Wu, L., Zuo, C., Zhang, H.: 'A cloud model based fruit fly optimization algorithm', *Knowl.-Based Syst.*, 2015, **89**, pp. 603–617

[13] Pan, Q.K., Sang, H.Y., Duan, J.H., *et al.*: 'An improved fruit fly optimization algorithm for continuous function optimization problems', *Knowl.-Based Syst.*, 2014, **62**, pp. 69–83

[14] Shen, L., Chen, H., Yu, Z., *et al.*: 'Evolving support vector machines using fruit fly optimization for medical data classification', *Knowl.-Based Syst.*, 2016, **96**, pp. 61–75

[15] Ma, J., Theiler, J., Perkins, S.: 'Accurate on-line support vector regression', *Neural Comput.*, 2003, **15**, (11), pp. 2683–2703

[16] Su, H., Yu, S.: 'Hybrid GA based online support vector machine model for short-term traffic flow forecasting'. Int. Workshop on Advanced Parallel Processing Technologies, Guangzhou, China, 2007, pp. 743–752

[17] Huang, G.B., Zhu, Q.Y., Siew, C.K.: 'Extreme learning machine: a new learning scheme of feedforward neural networks'. 2004 IEEE Int. Joint Conf. Neural Networks, Budapest, Hungary, 2004, vol. **2**, pp. 985–990

[18] Huang, G.B., Siew, C.K.: 'Extreme learning machine with randomly assigned RBF kernels', *Int. J. Inf. Technol.*, 2005, **11**, (1), pp. 16–24

[19] Jiang, X., Adeli, H.: 'Dynamic wavelet neural network model for traffic flow forecasting', *J. Transp. Eng.*, 2005, **131**, (10), pp. 771–779

[20] Wang, J., Shi, Q.: 'Short-term traffic speed forecasting hybrid model based on chaos–wavelet analysis-support vector machine theory', *Transp. Res. C, Emerg. Technol.*, 2013, **27**, pp. 219–232